Computation of Log BB Values for Compounds Transported through Carrier-Mediated Mechanisms Using *in Vitro* Permeability Data from Brain Microvessel Endothelial Cell (BMEC) Monolayers

Helen H. Usansky[1] and Patrick J. Sinko[1,2]

Received September 20, 2002; accepted December 4, 2002

Purpose. To explore the possibility of determining *in vivo* log BB values (the logarithm value of brain to plasma concentration ratio) from *in vitro* permeability data measured in brain microvessel endothelial cell (BMEC) monolayers.

Methods. An equilibrium mathematical model was developed: log BB = $\log(C_a/C_b)$ + log $K_{br:pl}$, where C_b and C_a are the drug concentrations at equilibrium in the basolateral (B) and apical (A) sides of BMECs in an A-to-B directional diffusion system and $K_{br:pl}$ is the brain–plasma partition coefficient. With this model, murine log BB values were calculated for 24 pharmaceutical compounds, mostly *Pgp* substrates.

Results. Calculated log BB values correlated well to experimental values (r^2 = 0.854, slope = 0.907 ± 0.080), demonstrating that the model could reasonably predict brain penetration for compounds that are involved in carrier-mediated transport mechanisms. For a second data set that included volatile organic compounds (log BB = log $K_{br:pl}$), log $K_{br:pl}$ values were also shown to correlate well with their respective experimental log BB values (r^2 = 0.876, slope = 0.973 ± 0.082), demonstrating that log $K_{br:pl}$ is an excellent descriptor for log BB when a compound penetrates the blood–brain barrier by passive diffusion only.

Conclusion. The equilibrium model demonstrated a reasonable ability to compute *in vivo* log BB values, regardless of the involvement or mechanisms of carrier-mediated transport.

KEY WORDS: log BB; BBB permeability; BMEC monolayers; carrier-mediated transport; *Pgp* substrates.

INTRODUCTION

The blood–brain barrier (BBB) protects the brain by limiting the penetration of exogenous compounds. The ability to understand the penetration of drug candidates through the BBB is pivotal during drug development. It allows scientists to choose drug candidates that possess more selective pharmacologic properties with fewer side effects and toxicities. However, using *in vivo* methods to measure the logarithmic values of brain-to-plasma drug concentration ratios (log BB) in humans is not possible, and to do so in animal models is expensive and time consuming. In order to improve the efficiency of drug discovery and development and to facilitate high-throughput drug screening, many prediction methods for estimating log BB have been developed based on a drug's physicochemical properties such as molecular weight, octanol–water partition coefficient, molecular surface area, Gibbs free energy, and others (1–3). Many published methods allow for a reasonable prediction of log BB values for compounds that cross the BBB by passive diffusion. However, the prediction of log BB becomes less reliable when carrier-mediated transport in either direction is involved. In fact, it was observed that the BBB permeability of compounds that utilize absorptive transporters, such as glucose and phenylalanine, were higher than predicted values, whereas the permeability of molecules involved in secretory transport, such as vincristine, vinblastine, and digoxin, was lower than predicted values (4).

In vitro diffusion studies using BMECs, mostly bovine brain microvessel endothelial cells (BBMECs), provide an important tool for determining the permeability of a compound through the BBB and identifying the mechanism(s) of drug transport into and out of the brain. Through permeability studies, the involvement of directional carrier-mediated transport can be differentiated. However, there are many differences between *in vitro* diffusion models and *in vivo* BBB systems. Besides deviations in physiologic conditions (e.g., oxygen levels, ion composition, protein concentrations), a major difference between *in vitro* and *in vivo* systems is that the media surrounding the BBMEC monolayer and the BBB are different. In a diffusion system, a BMEC monolayer is soaked in a buffer on both sides, whereas *in vivo*, the BBB is sandwiched between plasma on the apical side and brain tissue on the basolateral side. The compositional differences in lipids and water between these two tissues have significant impact on drug distribution (5). Because of these differences, drug permeability determined from BMEC monolayers cannot be reliably used to quantitatively determine log BB values.

In this paper, an equilibrium model for determining log BB values from *in vitro* permeability data is developed. With this model, the log BB values of 24 pharmaceutical compounds, mostly *Pgp* substrates, in mice were calculated from their BMEC permeability data, and the results correlated well to their corresponding experimental log BB values, indicating that this model provides a reasonable degree of prediction for compounds absorbed by passive and carrier-mediated mechanisms.

METHODOLOGY

Model Development

Determination of Permeability by Passive Diffusion (P_p) and Carrier-Mediated Transport (P_c)

Experimentally observed apical-to-basolateral BMEC monolayer permeability data (P_m) account for carrier-mediated and passive diffusive transport pathways:

$$P_m = \frac{J_{\max}}{K_m + C_a} + P_p = P_c' + P_p \quad (1)$$

where $J_{\max}$ and K_m are the apparent maximal flux and apparent Michaelis–Menten constant resulting from transport by one or more carriers independent of direction, C_a is the apical side drug concentration, P_p is the passive diffusive per-

[1] Department of Pharmaceutics, Ernest Mario School of Pharmacy, Rutgers University, Piscataway, New Jersey 08854-8022.

[2] To whom correspondence should be addressed. (e-mail: sinko@rci.rutgers.edu)

0724-8741/03/0300-0390/0 © 2003 Plenum Publishing Corporation

meability (paracellular and transcellular) and P_c' is the observed (apparent) net carrier-mediated permeability. When $C_a << K_m$, $P_c' \approx J_{max}/K_m = P_c$ (intrinsic carrier-mediated permeability), and Eq. (1) can be written as:

$$P_m = P_c + P_p \tag{2}$$

P_c' and P_c can be greater than (net carrier transport into the brain), less than (net carrier transport out of brain) or equal to zero (diffusion only or equal directional carrier transport).

For compounds transported mainly by passive diffusion, BMEC permeability was previously found to correlate well with their octanol–water partition coefficients ($K_{oc:w}$) and molecular weights (MW) (6,7). The relationship can be expressed as

$$P_p = A * \log\left(\frac{K_{oc:w}}{\sqrt{MW}}\right) + B \tag{3}$$

where A and B constants. P_p can be estimated using eq. (3). P_c can then be determined from the difference between P_m and P_p.

Drug Concentration Ratio across BMEC Monolayers at Equilibrium

In a directional diffusion system, the flux from the donor side to the receiver side decreases as the concentration gradient decreases across the monolayer. At equilibrium ($dM/dt = 0$), $J_{net} = dM/(S*dt) = 0$, and

$$P_p(C_a - C_b) = -\frac{J_{max}C_a}{K_m + C_a} \tag{4}$$

where C_b is the concentration in the receiver chamber.

When $C_a << K_m$, Eq. (4) can be written as:

$$\frac{C_b}{C_a} = 1 + \frac{P_c}{P_p} = 1 + \frac{P_c'}{P_p} \tag{5}$$

When $C_a \approx K_m$, $P_c' = J_{max}/2K_m = 1/2P_c$. Therefore, Eq. (5) becomes

$$\frac{C_b}{C_a} = 1 + \frac{P_c}{P_p} = 1 + \frac{2P_c'}{P_p} \tag{6}$$

When $C_a >> K_m$, P_c' approaches zero, and C_b/C_a approaches unity.

Brain–Plasma Partition Coefficient ($K_{br:pl}$)

It is well known that drug distribution in a body is affected by the drug's solubility (8). An equilibrium blood–tissue partition coefficient, measured *in vitro* or calculated based on drug solubility and the water–lipid content in the blood and tissues, is believed to govern the relative distribution of a drug between tissues and blood (9). A method for calculating the brain–plasma partition coefficient using these elements has been proposed (5) and is described as follows:

$$K_{br:pl} = \frac{K_{vo:w}(V_{nt} + 0.3V_{pht}) + V_{wt} + 0.7V_{pht}}{K_{vo:w}(V_{np} + 0.3V_{php}) + V_{wp} + 0.7V_{php}} \tag{7}$$

where $K_{vo:w}$ is the vegetable oil–water partition coefficient; V_{nt}, V_{pht}, and V_{wt} are the fractional contents of neutral lipids, phospholipids, and water in wet brain tissue, respectively; and V_{np}, V_{php}, and V_{wp} are the fractional contents of neutral lipids, phospholipids, and water in plasma, respectively. $K_{vo:w}$ can be calculated from $K_{oc:w}$ (10).

Brain-to-Plasma Concentration Ratios (BB) and Log BB

C_b/C_a represents drug distribution across a BMEC monolayer in a diffusion system under equilibrium conditions. C_b/C_a, as measured in the *in vitro* diffusion system, is likely to be different from *in vivo* BB values because brain–plasma partitioning has not been accounted for. Therefore, the *in vivo* BB value is the product of C_b/C_a and $K_{br:pl.}$

Case 1: $C_a \approx C_{pl}$. When $C_a << K_m$, $P_c' = P_c$. For predicting BB values at similar C_{pl} compared to C_a, log BB can be determined by combining Eqs. (5) and (7):

$$log\ BB = log\left(1 + \frac{P_c}{P_p}\right) + log\ K_{br:pl} \tag{8}$$

From this equation, it can be seen that when a drug penetrates the BBB by passive diffusion only or when net carrier-mediated flux is zero (i.e., $P_c = 0$), the log BB equals log $K_{br:pl}$ consistent with the concept of the brain–plasma partition coefficient.

When $C_a \approx K_m$, $P_c' = 1/2P_c$. When $C_a >> K_m$, P_c' approaches zero. However, when $C_a \approx C_{pl}$, P_c' measured *in vitro* becomes similar to that *in vivo*. In this case, P_c in Eq. (8) can be directly replaced with P_c' for log BB calculations.

Case 2: $C_a \neq C_{pl}$. When $C_a \approx K_m$ and $C_{pl} << K_m$, log BB should be determined by combining Eqs. (6) and (7):

$$log\ BB = log\left(1 + \frac{2P_c'}{P_p}\right) + log\ K_{br:pl} \tag{9}$$

When $C_a << K_m$ and $C_{pl} \approx K_m$, log BB should be calculated with the following equation:

$$log\ BB = log\left(1 + \frac{P_c}{2P_p}\right) + log\ K_{br:pl} \tag{10}$$

When $C_a >> K_m$ and $C_{pl} << K_m$, P_c' observed *in vitro* approaches zero while P_c' *in vivo* equals P_c. Such a difference in Pc' data can cause inaccurate log BB prediction. When $C_a << K_m$ and $C_{pl} >> K_m$, log BB values can be directly estimated from log $K_{br:pl}$ because P_c' (*in vivo*) approaches zero at saturated C_{pl}.

Computational Methods

Very few literature reports present both P_m and log BB data. Because of this limitation, the log BB values from a group of organic solvent compounds were used to validate $K_{br:pl}$ (Table I); the P_m data from a group of diffusion markers and compounds without significant carrier-mediated involvement were used in evaluation of the linearity between P_p and $K_{oc:w}/MW^{0.5}$ (Table II); and finally, the compounds that have both experimental P_m and log BB data available were used as test compounds for the prediction of log BB (Table III).

Validation of $K_{br:pl}$

Organic solvent compounds with molecular weights less than 200 and log $K_{oc:w}$ values from –0.17 to 1.04 were selected to validate the calculation of $K_{br:pl}$ as a drug brain–plasma

Table I. Experimental Log BB Values of Organic Compounds and Their Corresponding Log $K_{br:pl}$ Data[a]

Compound	MW	Log $K_{oc:w}$	Exp log BB	Log $K_{br:pl}$	Exp BB/$K_{br:pl}$
Butanone	72.1	0.29	–0.08	–0.109	1.07
Benzene	78.1	2.13	0.37	0.093	1.89
3-Methylpentane	86.2	3.6	1.01	0.920	1.23
2-Propanol	60.1	0.05	–0.15	–0.110	0.91
2-Methylpropanol	74.1	0.76	–0.17	–0.103	0.86
2-Methylpentane	86.2	3.21	0.97	0.731	1.73
2,2-Dimethylbutane	86.2	3.82	1.04	0.990	1.12
1,1,1-Trichloroethane	133.4	2.49	0.4	0.271	1.35
Dicthyl ether	74.1	0.89	0	–0.100	1.26
Enflurane	184.5	2.1	0.24	0.081	1.44
Ethanol	46.1	–0.31	–0.16	–0.111	0.89
Halothane	197.4	2.3	0.35	0.168	1.52
Heptane	100.2	4.66	0.81	1.095	0.52
Hexane	86.2	3.9	0.8	1.010	0.62
Isoflurane	184.5	2.06	0.42	0.066	2.26
Methylcyclopentane	84.2	3.37	0.93	0.818	1.29
Pentane	72.1	3.39	0.76	0.828	0.85
Propanol	60.1	0.25	–0.16	–0.109	0.89
Propanone	58.1	–0.24	–0.15	–0.110	0.91
Teflurane	180.9	1.95	0.27	0.030	1.74
Toluene	92.1	2.73	0.37	0.421	0.89
Trichloroethene	131.4	2.42	0.34	0.231	1.28

[a] The Log $K_{oc:w}$ and experimental log BB data were taken from Luco (3).

distribution parameter. The rationales for choosing these compounds include their simplicities in chemical structure and transport mechanism through the BBB and their frequent use in training sets for establishing log BB prediction methods (2,3). Ether, ethanol and many volatile substances can freely pass through a plasma membrane and their blood-tissue distribution is dependent on their partial pressures in blood and solubility in the tissue (8). Their log BB values at equilibrium should be equal or close to their log $K_{br:pl}$ because these compounds pass through the BBB only by diffusion.

Based on this hypothesis, the log $K_{br:pl}$ values of these compounds were calculated using Eq. (7), and the results were compared with their experimental log BB values. The agreement between log $K_{br:pl}$ and experimental log BB values and their linear correlation were used for evaluating the significance and accuracy of $K_{br:pl}$ as a predictor of passive drug brain–plasma distribution at equilibrium.

Table II. Passive Diffusion Permeability in BMEC Monolayers and Related Chemical Properties[a]

Compound	MW	Log $K_{oc:w}$	Permeability (10^{-5} cm/s)
Sodium butyrate	110.1	–3.2[19]	1.29[6]
Sucrose	342.3	–3.7[19]	0.910[20]
Mannitol	182.2	–3.1[19]	1.66[21]
Glycerol	92.1	–2.42[6]	0.950[6]
Urea	60.1	–1.66[6]	4.30[6]
Thiourea	76.1	–1.08[19]	2.83[6]
Caffeine	194.2	–0.07[6]	6.72[6]
Propranolol	259.3	2.75[19]	11.5[6]
Estrone	270.4	3.13[19]	13.5[6]
Testosterone	288.4	3.32[19]	14.9[6]
Haloperidol	375.9	4.3[19]	16.2[6]
Progesterone	314.5	3.87[19]	14.8[6]

[a] $K_{oc,w}$ and permeability data were gathered from Refs. 6, 19–21. The superscripts in parentheses represent reference numbers.

Evaluation of the Relationship of P_p and $K_{oc:w}/MW^{0.5}$

Linear correlations between P_m and $K_{oc:w}/MW^{0.5}$ have been reported in numerous literature references (6,7). However, the compounds used in these correlations were not always representative of passive diffusion due to exclusion of compounds with a paracellular diffusion component to their transport and the inclusion of compounds with a significant carrier-mediated component. In order to establish an accurate relationship between P_p and $K_{oc:w}/MW^{0.5}$, a group of compounds that penetrate through the BBB by paracellular and transcellular diffusion but without significant involvement of carrier-mediated transport (6,11,12) were selected. For the purpose of this analysis, the permeabilities of these compounds through BMEC monolayers were considered to represent P_p. Through best-fit linear regression, the constants A and B in Eq. (3) were determined, and the results were used in further log BB calculations.

Experimental $K_{oc:w}$ values were obtained mainly from the SRC (Syracuse Research Corporation) PhysProp Database through a website provided by Cambridge Soft Corporation (http://chemfinder.cambridgesoft.com) (19). When $K_{oc:w}$ values were unavailable in literature, $K_{oc:buffer,\ pH\ 7.4}$ were used for the log BB calculations.

Calculation of Log BB

Compounds that have both P_m in BMECs and log BB data available in the literature were mostly *Pgp* substrates. P_p values of these test compounds were estimated using Eq. (3). The difference between P_m and P_p was considered as P_c. Since most P_m data from BMEC monolayers and experimen-

Table III. Experimental and Calculated Log BB Values of Pharmaceutic Compounds

Compound	Log $K_{oc:w}$	Exp P_m (10^{-5} cm/s)	Exp log BB	Calc. P_p (10^{-5}cm/s)	Calc. Log BB	Exp BB/ Calc BB
Acyclovir	–1.56[19]	1.04[6]	–0.836[22]c	3.92	–0.689	0.71
Antipyrine	0.38[19]	5.59 [7.27[6], 3.90[12]]	–0.097[3]	7.94	–0.261	1.46
Bunitrolol	1.6[19]	25.3[15]	0.38[15]c	10.3	0.344	1.09
Caffeine	–0.07[6]	7.69 [6.72[6], 8.85[12], 7.54[21]]	–0.0371 [–0.055[3], –0.0200[21]]	7.01	–0.0699	1.08
Cyclosporine A	2.02[4]	3.60[23]	–0.781 [–1.26[24]c, –0.559 [25]]	10.5	–0.410	0.43
Didanosine	–0.54[20]	1.39[20]	–0.372 [–1.3[26], –0.097[27]]	5.97	–0.745	2.36
Digoxin	1.73[4]	0.500[27]c	–1.230 [–1.1[24]c, –1.22[25], –1.43[28]]	10.0	–1.33	1.25
Doxorubicin	1.27[19]	1.32[29]	–0.83[30]c	9.28	–0.928	1.25
Flesinoxan	2.00[31]	3.16[32]c	–0.447[32]c	10.9	–0.491	1.11
Indinavir	2.79[20]	0.570[20]	–0.75[33]	12.3	–0.874	1.34
Nevirapine	1.81[34]	8.86[20]	0.00[1]	10.7	–0.0882	1.23
Phenytoin	2.47[19]	5.60[12]	–0.14 [–0.271[5]c, –0.04[2]]	12.1	–0.0738	0.86
Propranolol	2.75[19]	11.5[6]	0.64[2]	12.6	0.394	1.76
13-*cis*-Retinoic acid	6.74[19]	0.620[35]	–0.494[36]	20.7	–0.412	0.83
Ribavirin	–1.85[6]	0.683[6]	–0.668[37]c	3.29	–0.794	1.34
Saquinavir	4.51[20]	0.0650[20]	–0.948 [–1.03[38], –0.879[25]]	15.8	–1.30	2.24
Stavudine	–0.72[20]	1.17[20]	–0.48[34]	5.63	–0.793	2.06
Theophylline	–0.020[19]	3.90[12]	–0.29[3]	7.15	–0.373	1.21
Urea	–1.66[6]	4.30[6]	–0.142[39]	4.30	–0.111	0.93
Valproic acid	0.143[4]	4.50[12]	–0.22[3]	7.58	–0.336	1.30
Vinblastine	3.51[a]	0.968[b]	–0.0652 [–0.511[40], –0.22[41]c, 0.223[25]]	13.7	–0.266	1.59
Vincristine	2.80[7]	0.393[b]	–1.03 [–1.57[25], –1.18[42], –0.721[43]c]	12.2	–1.02	0.99
Zalcitabine	–1.1[20]	1.47[20]	–0.85[1]	4.88	–0.632	0.61
Zidovudine	0.044[19]	2.24 [2.75[44], 1.65[29]]	–0.72[20]	7.10	–0.611	0.78

Note: Experimental $K_{oc:w}$ and LogBB data were obtained from Refs. 1–7, 12, 15, 19–44. The superscripts in parentheses represent the reference numbers. When more than one value was available, mean values were used in the calculations and comparisons.

[a] CLogP.

[b] Unpublished data.

[c] Determined from graphic or related experimental data.

tal log BB data were observed in the low-micromolar (μM) range, log BB was calculated using Eq. (8) assuming that both C_a and $C_{pl} \leq K_m$ and $C_a \approx C_{pl}$.

Because most experimental log BB values in the literature were from mouse studies, $K_{br:pl}$ was calculated using the mouse values of V_{nt} (0.031), V_{pht} (0.05), V_{wt} (0.71), V_{np} (0.0026), V_{php} (0.0032), and V_{wp} (0.96), as reported in the literature (5). Based on estimated C_b/C_a and $K_{br:pl}$, mouse log BB values for test compounds were determined. The differences between calculated and experimental log BB values were compared, and their correlation was evaluated. Log $K_{br:pl}$ values for test compounds were also compared with corresponding experimental log BB data to examine the relationship of log $K_{br:pl}$ and log BB when carrier-mediated transport mechanism(s) was (were) involved in drug BBB penetration.

Some reported P_m values were expressed as milliliter per gram protein per second (ml/g protein/s). These data were converted to centimeters per second cm/s, assuming that the surface area of BBB equals 100 cm^2/g brain tissue protein (13). When brain and plasma concentration–time profiles were available, log BB values were determined as the brain–plasma concentration ratios at brain T_{max} (the time when drug concentration achieves its maximum in brain tissue).

Statistical Analysis

The significance of a linear regression was tested by analysis of variance (14) using Microsoft Excel 2000 (Microsoft Corp., Redmond, WA). Statistical significance level was defined as $p < 0.05$.

RESULTS

Calculated log $K_{br:pl}$ data for the solvent compounds were similar and correlated well to their corresponding experimental log BB data, with the ratio of experimental BB/calculated BB being 1.21 ± 0.43 and $r^2 = 0.876$ (Fig. 1). The similarity and excellent correlation between log $K_{br:pl}$ and experimental log BB values demonstrate that log $K_{br:pl}$ can represent log BB values at equilibrium for compounds that cross the BBB only by passive diffusion. As expected, this result reaffirms that drug distribution in the plasma and brain tissues is significantly governed by drug solubility and the lipid–water composition of tissues.

In contrast, the calculated log $K_{br:pl}$ values for the test compounds correlated poorly to their experimental log BB data ($r^2 = 0.0022$, Fig. 2), indicating that log $K_{br:pl}$ values alone can not be used to determine log BB values when carrier-mediated mechanisms are involved in drug penetration of the BBB.

The linear correlation between P_p and log ($K_{oc:w}/MW^{0.5}$) is illustrated in Fig. 3. The excellent correlation ($r^2 = 0.963$) reconfirms that drug solubility and molecular size are significant determinants of passive diffusion across BMEC monolayers.

Estimated P_p values for the test compounds range from

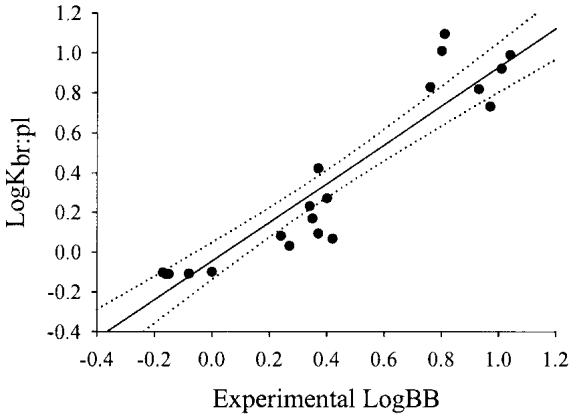

Fig. 1. Linear correlation of the experimental log BB values of organic compounds vs. their log $K_{br:pl}$ values: log$K_{br:pl}$ = 0.973 (± 0.082) exp log BB – 0.0445 (± 0.0458); r^2 = 0.876, Sŷ = 0.160, F = 141, df = 20, SSreg = 3.62, SSresid = 0.513 ($p < 0.01$). *Dotted lines* indicate 95% confidence intervals in regression.

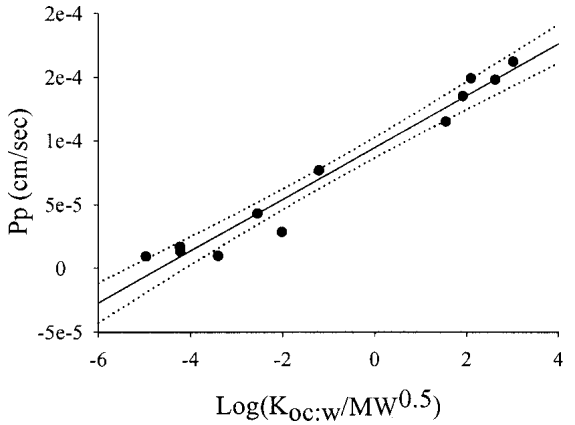

Fig. 3. Correlation of passive diffusion (P_p) through brain microvessel endothelial cell monolayer and compounds' chemical properties [log ($K_{oc:w}/MW^{0.5}$)]. P_p (10^{-5} cm/s) = 2.033 (± 0.125) log ($K_{oc:w}/MW^{0.5}$) + 9.48 (± 0.38), r^2 = 0.963, Sŷ = 1.25×10^{-5}, F = 263, df = 10, SSreg = 4.11×10^{-8}, SSresid = 1.56×10^{-9} ($p < 0.01$). *Dotted lines* indicate 95% confidence intervals in regression.

3.29 to 20.7 ($\times 10^{-5}$) cm/s (Table III). The C_b/C_a values for most *Pgp* substrates were less than 1, except for bunitrolol (2.46). $K_{br:pl}$ values calculated using Eq. (6) were highly dependent on the lipophilicity of test compounds, with the lowest value being 0.774 (didanosine) and the highest being 12.9 (13-*cis*-retinoic acid). Calculated log BB values were generally less than zero, indicating that for most compounds brain concentrations were less than plasma concentrations at equilibrium. Calculated log BB values were nearly identical to their corresponding experimental values (experimental BB/calculated BB = 1.24 ± 0.49) with reasonable linear correlation (r^2 = 0.854 and slope = 0.907 ± 0.080, Fig. 4), demonstrating that the current equilibrium log BB model can quantitatively estimate *in vivo* log BB values from *in vitro* P_m data with reasonable accuracy for this limited data set.

DISCUSSION

Prediction of log BB is pivotal in drug development. The common use of *in vitro* based BMEC diffusion model systems provides important information regarding drug permeability and transport mechanisms across the BBB. In this paper, an equilibrium model was developed, and its usefulness for the quantitative determination of murine *in vivo* log BB from *in vitro* BMEC P_m was evaluated.

The excellent linear correlation between BMEC permeabilities of the compounds that penetrate the BBB mainly by diffusion and their log ($K_{oc:w}/MW^{0.5}$) reaffirms that passive drug diffusion through BMECs is primarily governed by its lipophilicity and molecular size. Through such a relationship, P_p becomes calculable and can be differentiated from P_c. Estimated P_c values for most *Pgp* substrates were negative (data not shown), demonstrating the sensitivity of the model. The P_c value for bunitrolol, a β-blocker, was positive. Although it has been confirmed as a *Pgp* substrate (15), bunitrolol may also be a substrate for other transporters as well. For instance, some β-blockers such as propanolol and metoprolol have been found to be substrates for OCT-2, a transporter that facilitates transport across the apical membrane of an epithelial cell in the lungs and kidneys (16). In this equi-

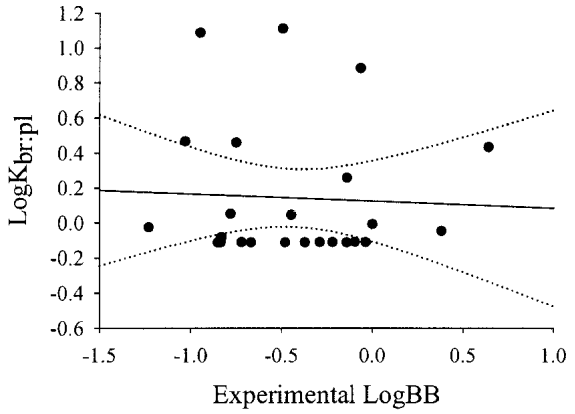

Fig. 2. Linear correlation of the experimental log BB values from the test pharmaceutic compounds vs. their log $K_{br:pl}$ values: log $K_{br:pl}$ = –0.0407 (± 0.1838) exp log BB + 0.125 (± 0.114). r^2 = 0.00222, Sŷ = 0.401, F = 0.0490, df = 22, SSreg = 0.00788, SSresid = 3.53 ($p > 0.05$). *Dotted lines* indicate 95% confidence intervals in regression.

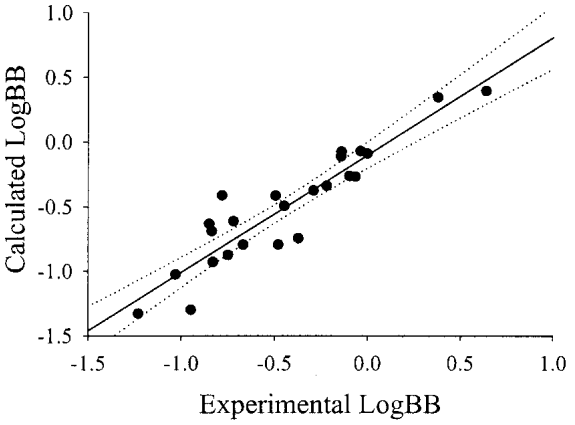

Fig. 4. Linear correlation of the experimental log BB values from the test pharmaceutic compounds versus the calculated log BB values: calc. log BB = 0.907 (± 0.080) exp log BB – 0.101 (± 0.050), r^2 = 0.854, Sŷ = 0.175, F = 128, df = 22, SSreg = 3.92, SSresid = 0.671 ($p < 0.01$). *Dotted lines* indicate 95% confidence intervals in regression.

librium model, P_c is the net result of carrier-mediated transport without differentiation of one particular transport mechanism or direction from another.

There is a greater than twofold difference between the calculated and observed log BB data for some compounds such as saquinavir and cyclosporine A. The accuracy of the calculated log BB values depends on the accuracy of experimental P_m and $K_{oc:w}$ data. The consistency between calculated and experimental log BB depends on the accuracy of these two values. With limited data available in literature, it was difficult to judge the accuracy of reported P_m, $K_{oc:w}$, and log BB. Therefore, when available, the mean experimental P_m values were used as the raw data for the log BB calculations, and the mean experimental log BB values were used in the comparisons with the calculated values. Very little kinetic data exist for absorptive carrier-mediated compounds (i.e., experimental log BB in mice or P_m data in BMEC could not always be found in literature). Because of this, the comparison between the calculated and experimental log BB values for the compounds involved in absorptive carriers through BBB could not be evaluated.

The accuracy of the calculated log BB values using the equilibrium model reveals that the brain-to-plasma concentration ratio of a compound is controlled by both transport mechanism(s) and the water–lipid composition in these two tissues. *In vitro* P_m and C_b/C_a at equilibrium can be used as indicators for how rapidly a drug can penetrate into brain tissue and which directional transport pathway is the dominating mechanism. However, without the introduction of $K_{br:pl}$ into the model, quantitative determination of log BB can not be achieved. On the other hand, $K_{br:pl}$ alone can be used to compute log BB only for compounds that pass through the BBB solely by passive diffusion. For compounds involved in absorptive, secretory, or a combination of carrier-mediated transport mechanisms, experimental log BB poorly correlated to log $K_{br:pl}$, indicating that both $K_{br:pl}$ and C_b/C_a at equilibrium are important determinants in log BB calculations when a carrier-mediated transport mechanism is involved in drug BBB penetration. The current model does not allow for the discrimination of multiple directional carrier-mediated transport pathways. Rather, it lumps the carrier-mediated pathways together to give a sense of net carrier-mediated transport (i.e., which direction dominates the overall carrier-mediated component of total transport). This is useful in early drug discovery, when mechanistic assessments are not as critical to drug development decisions. However, later in the development cycle, more mechanistic insight may be needed.

Without precise definition, log BB values can be misleading and even meaningless. That is because log BB values can vary from zero to infinity as a result of differences in absorption or/and elimination rates in the brain and plasma. However, if the rates in both tissues are the same, the log BB values remain constant throughout the entire concentration–time course. Otherwise, the log BB values need to be specified with time. In the current model, log BB determination is restricted to the concentration ratios when brain drug concentration achieves its maximum. At this moment, drug flux into brain tissue is equal to that out of brain tissue ($Flux_{in} = Flux_{out}$), which is consistent with the equilibrium condition of the model.

Usually, the elimination rates in brain and plasma are similar. In this case, the equilibrium model can also be extended to determine the concentration ratios during the entire elimination phase. However, in some cases the elimination rates in both tissues can be completely different, as seen for digoxin and ivermectin in *Pgp* knockout mice (17,18). In these cases, log BB determination using the equilibrium model should be based on the P_m data obtained from *Pgp*-deficient BMECs, and the predicted log BB applies only to the concentration ratio at T_{max} in brain tissue.

The log BB equilibrium model developed in this paper is species-specific. With relevant $K_{br:pl}$ data, this model can be used to predict log BB values in other species, such as human. This model can also be extended for predicting blood–tissue concentration ratio across other blood–tissue barriers such as blood–placenta, blood–testis, etc., with appropriate P_m data and relevant blood–tissue partition coefficients. However, the extension of this model to other tissues should be carefully evaluated because of the differences in the features of drug transport between BBB and other blood–tissue barriers.

CONCLUSIONS

The equilibrium model demonstrated a relationship between *in vitro* permeability in BMECs and log BB values, and revealed the importance of both BMEC permeability data and tissue lipid–water composition. With this model, *in vivo* log BB can be quantitatively determined from *in vitro* BMEC P_m data, regardless of the involvement of the type or directionality of the transport mechanisms.

ACKNOWLEDGMENT

We thank Ms. Peidi Hu for her contribution in gathering experimental log BB data.

REFERENCES

1. M. Feher, E. Sourial, and J. M. Schmidt. A simple model for the prediction of blood–brain partitioning. *Int. J. Pharm.* **201**:239–247 (2000).
2. J. A. Platts, M. H. Abraham, Y. H. Zhao, A. Hersey, L. Ijaz, and D. Butina. Correlation and prediction of a large blood–brain distribution data set—an LFER study. *Eur. J. Med. Chem.* **36**:719–730 (2001).
3. J. M. Luco. Prediction of the brain–blood distribution of a large set of drugs from structurally derived descriptors using partial least-squares (PLS) modeling. *J. Chem. Inf. Comput. Sci.* **39**:396–404 (1999).
4. H. Murakami, H. Takanaga, H. Matsuo, H. Ohtani, and Y. Sawada. Comparison of blood–brain barrier permeability in mice and rats using *in situ* brain perfusion technique. *Am. J. Physiol. Heart Circ. Physiol.* **279**:H1022–H1028 (2000).
5. P. Poulin and F. P. Theil. A priori prediction of tissue:plasma partition coefficients of drugs to facilitate the use of physiologically-based pharmacokinetic models in drug discovery. *J. Pharm. Sci.* **89**:16–35 (2000).
6. M. V. Shah, K. L. Audus, and R. T. Borchardt. The application of bovine brain microvessel endothelial-cell monolayers grown onto polycarbonate membranes *in vitro* to estimate the potential permeability of solutes through the blood–brain barrier. *Pharm. Res.* **6**:624–627 (1989).
7. V. A. Levin. Relationship of octanol/water partition coefficient and molecular weight to rat brain capillary permeability. *J. Med. Chem.* **23**:682–684 (1980).
8. S. K. Kennedy and D. E. Longnecker. History and principles of anesthesiology. In J. G. Hardman, A. G. Gilman, and L. E. Limbird (eds.), *Goodman & Gilman's The Pharmacological Basis of Therapeutics*, McGraw-Hill, New York, 1996, pp. 682–684.
9. P. Poulin and K. Krishnan. A biologically-based algorithm for

predicting human tissue: blood partition coefficients of organic chemicals. *Hum. Exp. Toxicol.* **14**:273–280 (1995).
10. A. Leo, C. Hansch, and D. Elkins. Partitioning coefficients and their uses. *Chem. Rev.* **71**:525–616 (1971).
11. M. D. Johnson and B. D. Anderson. *In vitro* models of the blood–brain barrier to polar permeants: comparison of transmonolayer flux measurements and cell uptake kinetics using cultured cerebral capillary endothelial cells. *J. Pharm. Sci.* **88**:620–625 (1999).
12. K. W. Otis, M. L. Avery, S. M. Broward-Partin, D. K. Hansen, H. W. Behlow, Jr., D. O. Scott, and T. N. Thompson. Evaluation of the BBMEC model for screening the CNS permeability of drugs. *J. Pharmacol. Toxicol. Methods* **45**:71–77 (2001).
13. U. Bickel, T. Yoshikawa, and W. M. Pardridge. Delivery of peptides and proteins through the blood–brain barrier. *Adv. Drug Deliv. Rev.* **46**:247–279 (2001).
14. J. H. Zar. *Biostatistical Analysis*, Prentice Hall, Englewood Cliffs, New Jersey, 1984.
15. J. Matsuzaki, C. Yamamoto, T. Miyama, H. Takanaga, H. Matsuo, H. Ishizuka, Y. Kawahara, M. Kuwano, M. Naito, T. Tsuruo, and Y. Sawada. Contribution of P-glycoprotein to bunitrolol efflux across blood–brain barrier. *Biopharm. Drug Dispos.* **20**:85–90 (1999).
16. A. J. Dudley, K. Bleasby, and C. D. Brown. The organic cation transporter OCT2 mediates the uptake of beta-adrenoceptor antagonists across the apical membrane of renal LLC-PK(1) cell monolayers. *Br. J. Pharmacol.* **131**:71–79 (2000).
17. U. Mayer, E. Wagenaar, J. H. Beijnen, J. W. Smit, D. K. Meijer, J. van Asperen, P. Borst, and A. H. Schinkel. Substantial excretion of digoxin via the intestinal mucosa and prevention of long-term digoxin accumulation in the brain by the mdr 1a P-glycoprotein. *Br. J. Pharmacol.* **119**:1038–1044 (1996).
18. A. H. Schinkel, J. J. Smit, O. van Tellingen, J. H. Beijnen, E. Wagenaar, L. van Deemter, C. A. Mol, M. A. van der Valk, E. C. Robanus-Maandag, and H. P. te Riele. Disruption of the mouse mdr1a P-glycoprotein gene leads to a deficiency in the blood–brain barrier and to increased sensitivity to drugs. *Cell* **77**:491–502 (1994).
19. SRC PhysProp Database. (http://chemfinder.cambridgesoft.com).
20. S. L. Glynn and M. Yazdanian. *In vitro* blood–brain barrier permeability of nevirapine compared to other HIV antiretroviral agents. *J. Pharm. Sci.* **87**:306–310 (1998).
21. D. K. Hansen, D. O. Scott, K. W. Otis, and S. M. Lunte. Comparison of *in vitro* BBMEC permeability and *in vivo* CNS uptake by microdialysis sampling. *J. Pharm. Biomed. Anal.* **27**:945–958 (2002).
22. P. de Miranda, H. C. Krasny, D. A. Page, and G. B. Elion. The disposition of acyclovir in different species. *J. Pharmacol. Exp. Ther.* **219**:309–315 (1981).
23. R. Cecchelli, B. Dehouck, L. Descamps, L. Fenart, V. Buee-Scherrer, V, C. Duhem, S. Lundquist, M. Rentfel, G. Torpier, and M. P. Dehouck. *In vitro* model for evaluating drug transport across the blood–brain barrier. *Adv. Drug Deliv. Rev.* **36**:165–178 (1999).
24. A. Tsuji and I. Tamai. Carrier-mediated or specialized transport of drugs across the blood–brain barrier. *Adv. Drug Deliv. Rev.* **36**:277–290 (1999).
25. I. Tamai and A. Tsuji. Transporter-mediated permeation of drugs across the blood–brain barrier. *J. Pharm. Sci.* **89**:1371–1388 (2000).
26. B. D. Anderson, B. L. Hoesterey, D. C. Baker, and R. E. Galinsky. Uptake kinetics of 2′,3′-dideoxyinosine into brain and cerebrospinal fluid of rats: intravenous infusion studies. *J. Pharmacol. Exp. Ther.* **253**:113–118 (1990).
27. H. J. Kang, M. G. Wientjes, and J. L. Au. Physiologically based pharmacokinetic models of 2′,3′-dideoxyinosine. *Pharm. Res.* **14**: 337–344 (1997).
28. E. V. Batrakova, D. W. Miller, S. Li, V. Y. Alakhov, A. V. Kabanov, and W. F. Elmquist. Pluronic P85 enhances the delivery of digoxin to the brain: *in vitro* and *in vivo* studies. *J. Pharmacol. Exp. Ther.* **296**:551–557 (2001).
29. E. V. Batrakova, S. Li, D. W. Miller, and A. V. Kabanov. Pluronic P85 increases permeability of a broad spectrum of drugs in polarized BBMEC and Caco-2 cell monolayers. *Pharm. Res.* **16**:1366–1372 (1999).
30. C. Rousselle, P. Clair, J. M. Lefauconnier, M. Kaczorek, J. M. Scherrmann, and J. Temsamani. New advances in the transport of doxorubicin through the blood–brain barrier by a peptide vector-mediated strategy. *Mol. Pharmacol.* **57**:679–686 (2000).
31. W. Kuipers, C. G. Kruse, W. van I. P. J. Standaar, M. T. Tulp, N. Veldman, A. L. Spek, and A. P. IJzerman. 5-HT_{1A}-versus D_2-receptor selectivity of flesinoxan and analogous N4-substituted N1-arylpiperazines. *J. Med. Chem.* **40**:300–312 (1997).
32. D. S. van I. R. Smolders, L. Nabulsi, K. P. Zuideveld, A. G. de Boer, and D. D. Breimer. Active efflux of the 5-HT(1A) receptor agonist flesinoxan via P-glycoprotein at the blood–brain barrier. *Eur. J. Pharm. Sci.* **14**:81–86 (2001).
33. J. H. Lin, M. Chiba, S. K. Balani, I. W. Chen, G. Y. Kwei, K. J. Vastag, and J. A. Nishime. Species differences in the pharmacokinetics and metabolism of indinavir, a potent human immunodeficiency virus protease inhibitor. *Drug Metab. Dispos.* **24**:1111–1120 (1996).
34. M. Yazdanian. Blood–brain barrier properties of human immunodeficiency virus antiretrovirals. *J. Pharm. Sci.* **88**:950–954 (1999).
35. H. Franke, H. Galla, and C. T. Beuckmann. Primary cultures of brain microvessel endothelial cells: a valid and flexible model to study drug transport through the blood–brain barrier *in vitro*. *Brain Res. Brain Res. Protoc.* **5**:248–256 (2000).
36. C. C. Wang, S. Campbell, R. L. Furner, and D. L. Hill. Disposition of all-*trans*- and 13-*cis*-retinoic acids and *n*-hydroxyethylretinamide in mice after intravenous administration. *Drug Metab. Dispos.* **8**:8–11 (1980).
37. B. E. Gilbert and P. R. Wyde. Pharmacokinetics of ribavirin aerosol in mice. *Antimicrob. Agents Chemother.* **32**:117–121 (1988).
38. C. B. Washington, H. R. Wiltshire, M. Man, T. Moy, S. R. Harris, E. Worth, P. Weigl, Z. Liang, D. Hall, L. Marriott, and T. F. Blaschke. The disposition of saquinavir in normal and P-glycoprotein deficient mice, rats, and in cultured cells. *Drug Metab. Dispos.* **28**:1058–1062 (2000).
39. S. I. Rapoport, R. Fitzhugh, K. D. Pettigrew, U. Sundaram, and K. Ohno. Drug entry into and distribution within brain and cerebrospinal fluid: [^{14}C]urea pharmacokinetics. *Am. J. Physiol.* **242**:R339–R348 (1982).
40. E. Lyubimov, L. B. Lan, I. Pashinsky, and W. D. Stein. Effect of modulators of the multidrug resistance pump on the distribution of vinblastine in tissues of the mouse. *Anticancer Drugs* **7**:60–69 (1996).
41. J. van Asperen, A. H. Schinkel, J. H. Beijnen, W. J. Nooijen, P. Borst, and O. van Tellingen. Altered pharmacokinetics of vinblastine in Mdr1a P-glycoprotein-deficient Mice. *J. Natl. Cancer Inst.* **88**:994–999 (1996).
42. S. M. El Dareer, V. M. White, F. P. Chen, L. B. Mellet, and D. L. Hill. Distribution and metabolism of vincristine in mice, rats, dogs, and monkeys. *Cancer Treat. Rep.* **61**:1269–1277 (1977).
43. Y. Mitsunaga, H. Takanaga, H. Matsuo, M. Naito, T. Tsuruo, H. Ohtani, and Y. Sawada. Effect of bioflavonoids on vincristine transport across blood–brain barrier. *Eur. J. Pharmacol.* **395**:193–201 (2000).
44. R. Masereeuw, U. Jaehde, M. W. Langemeijer, A. G. de Boer, and D. D. Breimer. *In vitro* and *in vivo* transport of zidovudine (AZT) across the blood–brain barrier and the effect of transport inhibitors. *Pharm. Res.* **11**:324–330 (1994).